



Article

Optimization of a Method for Detecting Intracellular Sulfane Sulfur Levels and Evaluation of Reagents That Affect the Levels in *Escherichia coli*

Qiaoli Yu ¹, Mingxue Ran ¹, Yuqing Yang ¹, Huaiwei Liu ¹ , Luying Xun ^{1,2,*} and Yongzhen Xia ^{1,*}

¹ State Key Laboratory of Microbial Technology, Shandong University, 72 Binhai Road, Qingdao 266237, China; yuqiaoli@mail.sdu.edu.cn (Q.Y.); ranmx@sdu.edu.cn (M.R.); angyuq@mail.sdu.edu.cn (Y.Y.); liuhuawei@email.sdu.edu.cn (H.L.)

² School of Molecular Biosciences, Washington State University, Pullman, WA 99164-7520, USA

* Correspondence: luying_xun@vetmed.wsu.edu (L.X.); xiayongzhen2002@email.sdu.edu.cn (Y.X.); Tel.: +1-509-335-2787 (L.X.); +86-532-58631572 (Y.X.)

Abstract: Sulfane sulfur is a class of compounds containing zero-valent sulfur. Most sulfane sulfur compounds are reactive and play important signaling roles. Key enzymes involved in the production and metabolism of sulfane sulfur have been characterized; however, little is known about how to change intracellular sulfane sulfur (iSS) levels. To accurately measure iSS, we optimized a previously reported method, in which reactive iSS reacts with sulfite to produce thiosulfate, a stable sulfane sulfur compound, before detection. With the improved method, several factors were tested to influence iSS in *Escherichia coli*. Temperature, pH, and osmotic pressure showed little effect. At commonly used concentrations, most tested oxidants, including hydrogen peroxide, tert-butyl hydroperoxide, hypochlorous acid, and diamide, did not affect iSS, but carbonyl cyanide m-chlorophenyl hydrazone increased iSS. For reductants, 10 mM dithiothreitol significantly decreased iSS, but tris(2-carboxyethyl)phosphine did not. Among different sulfur-bearing compounds, NaHS, cysteine, S₂O₃²⁻ and diallyl disulfide increased iSS, of which only S₂O₃²⁻ did not inhibit *E. coli* growth at 10 mM or less. Thus, with the improved method, we have identified reagents that may be used to change iSS in *E. coli* and other organisms, providing tools to further study the physiological functions of iSS.

Keywords: intracellular sulfane sulfur; thiosulfate; redox homeostasis; sulfur-bearing compounds; *Escherichia coli*



Citation: Yu, Q.; Ran, M.; Yang, Y.; Liu, H.; Xun, L.; Xia, Y. Optimization of a Method for Detecting Intracellular Sulfane Sulfur Levels and Evaluation of Reagents That Affect the Levels in *Escherichia coli*. *Antioxidants* **2022**, *11*, 1292. <https://doi.org/10.3390/antiox11071292>

Academic Editor: Eizo Marutani

Received: 1 June 2022

Accepted: 24 June 2022

Published: 29 June 2022

Publisher's Note: MDPI stays neutral with regard to jurisdictional claims in published maps and institutional affiliations.



Copyright: © 2022 by the authors. Licensee MDPI, Basel, Switzerland. This article is an open access article distributed under the terms and conditions of the Creative Commons Attribution (CC BY) license (<https://creativecommons.org/licenses/by/4.0/>).

1. Introduction

Sulfide (H₂S and HS⁻) is considered the third gaso-transmitter in mammals, participating in various physiological functions [1,2]. Recent reports show that sulfide signaling is usually via intracellular sulfane sulfur (iSS) [3,4]. Sulfane sulfur, containing zero-valence sulfur, comes in several forms, such as inorganic and organic polysulfide (HS_n⁻, RS_n⁻, and RSS_nR; n ≥ 2) and elemental sulfur [5]. It modifies protein cysteine (Cys) thiols to form persulfide (S-sulfhydration), which alters protein configurations and amends the catalytic or regulatory activities [6]. Glyceraldehyde-3-phosphate dehydrogenases in *Escherichia coli* and *Staphylococcus aureus* are inhibited after their active site Cys residues are S-sulfhydrated [7,8], but the enzyme activity from the mouse liver is enhanced after S-sulfhydration [9]. Several bacterial gene regulators have been identified to respond to iSS. MgrA senses iSS after sulfide-stress to activate the expression of virulent factors in *S. aureus* [8]. The iSS level in *Pseudomonas aeruginosa* is high in the late log phase and early stationary phase of growth, and it activates MexR to turn on the expression of a multiple drug efflux pump MexAB when cells enter the stationary phase [10]. The high levels of iSS in the late log phase and early stationary phase of growth also significantly enhance the

activity of the master quorum-sensing activator LasR in *P. aeruginosa* [11]. The multidrug repressor MarR is inactivated by increased iSS in the early stationary phase of growth of *E. coli* [12]. When iSS is high, it modifies the oxidative stress regulator OxyR that activates the expression of genes involved in lowering iSS in *E. coli* [13]. Hence, iSS in bacteria also plays a critical role in regulating different physiological processes.

The iSS is unstable, as it can be oxidized by oxygen, reduced by thiols, and decomposed under acid conditions [14,15]. Therefore, the growth conditions and oxidative and reducing agents may interfere with iSS in bacteria. The growth conditions include osmolarity, pH, temperature, and dissolved oxygen [16–19]. Reactive oxygen species (ROS) cause oxidative stress [20,21], damaging proteins, nucleic acids, and lipids [22]. Superoxide radicals ($O_2^{\bullet-}$), hydrogen peroxide (H_2O_2), and hydroxyl radicals ($\bullet OH$) are common ROS, and they are produced via the electron transport chain of aerobic respiration [23]. Reagents, such as hypochlorous acid and carbonyl cyanide *m*-chlorophenyl hydrazone (CCCP), are often used to induce oxidative stress in cells. Hypochlorous acid is a strong oxidant, and it reacts with DNA, protein, and lipids [24]. CCCP is an uncoupling agent that inhibits oxidative phosphorylation and promotes ROS production [25], which induces oxidative stress in cells [26]. The reagents diamide and tert-butyl hydroperoxide (tBH) are common thiol oxidants [27]. Commonly used reducing agents include dithiothreitol (DTT) and tris(2-carboxyethyl)phosphine (TCEP). How these factors influence iSS levels in bacteria is unclear.

The production of iSS also affects its homeostasis. The metabolism of Cys is the main source of sulfane sulfur in *Escherichia coli* [28]. Cys is either present in a rich medium or is produced from sulfate [29]. Sulfate is reduced via assimilatory sulfate reduction to sulfide before being incorporated into Cys. The yeast *Saccharomyces cerevisiae* can convert thiosulfate to iSS which is then reduced to sulfide for Cys biosynthesis [30]. Further, the yeast *Schizosaccharomyces pombe* directly uses sulfane sulfur to produce Cys [31]. Garlic oil is rich in sulfane sulfur-containing compounds with diallyl disulfide (DADS) and diallyl trisulfide being prevalent [32]. The supply of these sulfur compounds in the growth medium may affect iSS.

Recently, we have developed a simple and sensitive method to detect total iSS from biological samples. SO_3^{2-} is used to react with unstable iSS to produce stable $S_2O_3^{2-}$ under hot and alkaline conditions (pH = 9.5, 95 °C). $S_2O_3^{2-}$ is then derived with monobromobimane (mBBBr) to form bimane- $S_2O_3^{2-}$, which is detected by using high-performance liquid chromatography (HPLC) with a fluorescence detector. The thiosulfate content of the samples incubated in the control buffer without sulfite is the blank sample that is subtracted from the test samples [33]. Thiosulfate is also a sulfane sulfur-containing compound [1], but it does not react with cellular thiols under physiological conditions [34,35]. This method was named as sulfite-dependent sulfane sulfur detection method (SdSS), and it is sensitive to detect active sulfane sulfur in bacteria, plants, and animals [10,31,33,36] as well as in wine [37].

However, after extensive use, we noticed several shortcomings that affect the accuracy and sensitivity of this method. The peaks of mBBBr derivatized $S_2O_3^{2-}$ and glutathione (GSH) partially overlapped, affecting the detection sensitivity of bimane- $S_2O_3^{2-}$; the washing process of preparing the bacterium samples might cause iSS loss; a fraction of iSS was converted to thiosulfate without sulfite during heating. Here, we addressed these issues and revised the method. With this improved method, we investigated the factors that could affect iSS in *E. coli*. The key findings included that thiosulfate is a good reagent to increase iSS without affecting bacterial growth.

2. Materials and Methods

2.1. Bacterial Strains, Culture Conditions, and Reagents

Escherichia coli BL21(DE3) was grown in the lysogeny broth (LB) at 37 °C. Sodium sulfite, sodium thiosulfate, sodium sulfate, GSH, Cys, NaHS, DTT, mBBBr, tBH, DADS, TCEP, diamide (CAS: 10465-78-8), and CCCP were purchased from Sigma-Aldrich (Burlington,

MA, USA). Diethylenetriaminepentaacetic acid (DTPA), $\text{FeSO}_4 \cdot 7\text{H}_2\text{O}$, acetic acid, sodium hypochlorite, and H_2O_2 were purchased from Bio Basic Inc (Markham, ON, Canada). TritonX-100 was purchased from Sangon Biotech (Shanghai, China). Rosup is a compound mixture of oxidative reagents, and it is used as a positive control in the Reactive Oxygen Species Assay Kit (Beyotime Biotech Inc., Shanghai, China).

2.2. Sample Preparations for iSS Detection

Colonies of *E. coli* BL21(DE3) were picked up and cultured in LB medium overnight. The cultures were transferred into a fresh medium at an initial OD_{600} of 0.05 for aerobic cultures or at an initial OD_{600} of 0.02 for anaerobic cultures. Cells were at defined time intervals, and the OD_{600} value was measured with the spectrophotometer UV1800 (Shimadzu, Kyoto, Japan). Three different procedures were used to harvest cells. Option 1 (No-wash): *E. coli* cells were transferred into a microfuge tube and harvested by centrifuging at $3300 \times g$ for 5 min at 4 °C. The supernatants were carefully removed with a pipettor, and the collected cells were used for iSS measurement. Option 2 (Double-centrifugation): after the cells were harvested and the supernatant was removed, the tubes with pellets were centrifuged again at $3300 \times g$ for 1 min. The residual supernatant was carefully removed with a pipettor. Option 3 (Wash-once): after the cells were harvested and the supernatant was removed, the collected pellets were washed once with 1 mL 100 mM Tris-HCl buffer (pH = 7.4) to remove the residual supernatant. Wash-once is the reported procedure [33]. No-wash and Double-centrifugation were two selected procedures for comparison. Double-centrifugation was found to be the optimal procedure and was adapted for iSS detection.

2.3. The Optimized iSS Detection Method

The previously reported SdSS method is designed to measure iSS [33]. The SdSS method was optimized. Briefly, the reaction buffer was prepared with 50 mM Tris-HCl buffer (pH = 9.5) containing 1% TritonX-100, 50 μM DTPA, and 1 mM sulfite, and the control buffer contained no sulfite but 0.5 mM DTT. DTT was introduced to reduce sulfate sulfur to H_2S , avoiding the spontaneous oxidation of sulfane sulfur to thiosulfate during subsequent steps. One mL of cells at OD_{600} of 1.0 was harvested with double-centrifugation and resuspended in 100 μL of the reaction buffer or the control buffer. The resuspended cells were incubated at 95 °C for 10 min. The samples were then centrifuged at $15,700 \times g$ for 3 min; 50 μL of the supernatant was mixed with 5 μL of 25 mM mBBr and incubated in the dark at room temperature for 25 min to convert $\text{S}_2\text{O}_3^{2-}$ into bimane- $\text{S}_2\text{O}_3^{2-}$ adduct. 110 μL of an acetic acid and acetonitrile mixture (*v/v*, 1:9) was added to stop the reaction and denature proteins. The mixtures were centrifuged to precipitate cell debris and denatured proteins at $15,700 \times g$ for 3 min.

The bimane- $\text{S}_2\text{O}_3^{2-}$ adduct in the supernatant was determined by using HPLC (LC-20A, Shimadzu, Kyoto, Japan) with a fluorescence detector (RF20A, Shimadzu, Kyoto, Japan). The gain value and sensitivity of this fluorescence detector were set as “medium” and “ $\times 16$ ”, respectively. Briefly, 5 μL supernatant was injected onto a reverse-phase C18 column (VP-ODS, 150×4 mm, Shimadzu, Kyoto, Japan) with a guard column (Inertsil ODS-SP 5 μm 5020-19006, Shimadzu, Kyoto, Japan) through an autosampler (SIL-20A, Shimadzu, Kyoto, Japan). The column was maintained at 38 °C in a column thermostat (CTO-20A, Kyoto, Japan), and eluted with a gradient solution A (0.25% acetic acid and 10% methanol in distilled water, with pH being adjusted to 3.9 by using NaOH) and solution B (0.25% acetic acid and 90% methanol in distilled water) from 8% B to 40% B in 7 min, 40% B for 5 min, 40% B to 100% in 0.1 min, 100% B for 6 min at a flow rate of 0.8 mL/min. The adduct was detected by a fluorescence detector with an optimized excitation wavelength (Ex) and emission wavelength (Em) at 380 nm and 466 nm, respectively. The bimane- $\text{S}_2\text{O}_3^{2-}$ adduct was normally detected at a retention time of 13.0 min.

2.4. The Effect of Growth Conditions and Reagents on *E. coli* iSS

The cells of *E. coli* BL21(DE3) were transferred into a fresh LB medium and incubated at 37 °C until OD₆₀₀ reached about 1.0. The cultures were aliquoted and incubated under various conditions, including different temperatures, pH, and osmolarities, or spiked with sulfur-containing compounds (NaHS, sulfite, sulfate, Cys, thiosulfate, DADS, and GSH), oxidants (H₂O₂, tBH, CCCP, diamide, sodium hypochlorite, Rosup, and Fenton's reagent) and reductants (DTT and TCEP). DADS and CCCP were dissolved in absolute ethanol and DMSO, respectively. The other reagents were dissolved in distilled water. Fenton reagent was prepared by mixing 10 mM H₂O₂ with 10 mM FeSO₄·7H₂O. The final concentration of each reagent was given in the results. After incubation for 30 min or as specified in the text [33], the cells were collected by using the double-centrifugation method and analyzed with our optimized SdSS method.

The iSS content in *E. coli* cells was also assayed with cells cultured under aerobic and anaerobic conditions. For aerobic growth, the cells were cultured in 50 mL of LB medium. For anaerobic growth, the cells were cultured in 100 mL serum bottles sealed with butyl rubber stoppers. 70 mL nitrogen deoxygenated LB medium was filled into the bottles before sterilization. The cells were inoculated in the bottles by using a syringe. Cells were taken at defined time intervals given in the results. The iSS content was detected by using our optimized method.

3. Results

The detection sensitivity for sulfane sulfur was improved by optimizing HPLC conditions. Sulfane sulfur is converted to S₂O₃²⁻, which is derivatized with mBBr to bimane-S₂O₃²⁻ for detection [33]; however, the peaks of mBBr-derivatized S₂O₃²⁻ and GSH partially overlapped within the chromatogram (Figure 1A). The HPLC elution program was optimized to separate the two peaks (Figure 1B). The maximal Ex and Em of bimane-S₂O₃²⁻ were determined to be 380 nm and 466 nm, respectively (Figure 2A,B). When the maximal wavelengths were used, the peak area of bimane-S₂O₃²⁻ increased about 20.0% over that obtained with the reported Ex and Em (Figure 2C). Nine combinations of the settings of gain value and sensitivity of the fluorescence detector were tested to increase the signal-to-noise ratio (SNR) for the bimane-S₂O₃²⁻ adduct (Table S1), and the highest value of the SNR was when the gain value was “×16” and the sensitivity was “medium”.

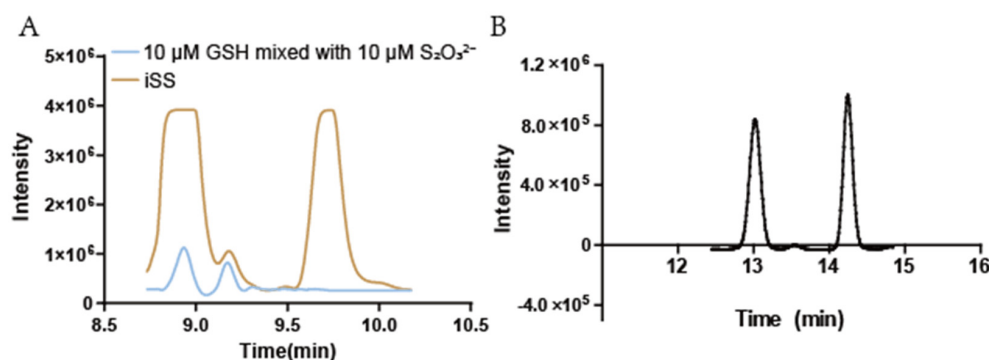


Figure 1. Partial HPLC chromatograms with two programs. The *E. coli* BL21(DE3) was cultured until the OD₆₀₀ reached around 1.0. The cells equivalent to 3 mL at OD₆₀₀ = 1 were collected and the iSS contents were determined with the SdSS method. After derivation with mBBr, the derivatives were determined with two different HPLC programs. (A) The previous used HPLC elution. The bimane-S₂O₃²⁻ (at 9.2 min) formed a peak overlapped with bimane-GSH (at 8.9 min). The blue curve was the mixture of 10 μM bimane-S₂O₃²⁻ and 10 μM bimane-GSH, which was routinely used as standard. The yellow curve was the mBBr-derivatives of an *E. coli* cell lysate. The large peak of bimane-GSH from the cell lysate overlapped with that of bimane-S₂O₃²⁻. (B) The optimized HPLC elution. The optimized elution separated bimane-GSH (at 10.5 min, not shown) and bimane-S₂O₃²⁻ (at 13.0 min).

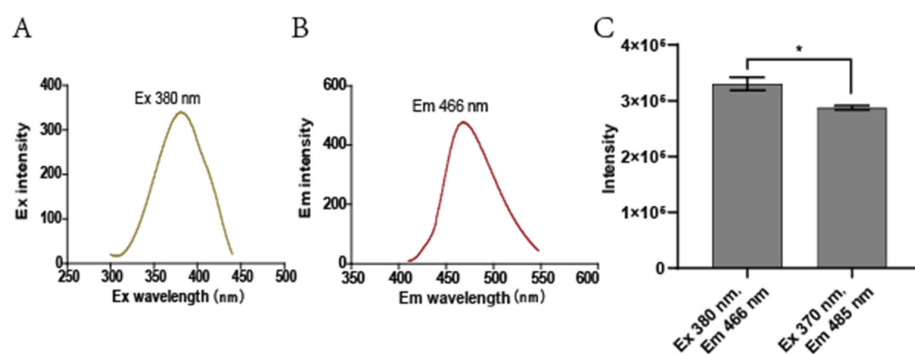


Figure 2. The optimal excitation and emission wavelengths of bimane- $S_2O_3^{2-}$. 0.05 mM $S_2O_3^{2-}$ was reacted with 0.25 mM mBBR to ensure $S_2O_3^{2-}$ was converted to bimane- $S_2O_3^{2-}$. This reaction solution was used to search for the optimal excitation and emission wavelengths. (A) Fixed Em at 485 nm to screen the Ex from 300 nm to 440 nm. (B) Fixed Ex at 370 nm to screen the Em from 410 nm to 550 nm. (C) The comparison of the peak area of bimane- $S_2O_3^{2-}$ detected with the optimized and original fluorescence detection parameters, respectively. Three parallel experiments were performed to obtain the averages and standard deviations ($n = 3$). A t -test was performed to calculate the p -value. Symbol * was shown when $p < 0.05$.

By using the optimized HPLC conditions, the standard curves of bimane- $S_2O_3^{2-}$ ranging from 0.5 μ M to 5 μ M in 50 mM Tris-HCl buffer (pH = 9.5) with or without *E. coli* BL21(DE3) at OD_{600} of 1.0 was determined. With the cells, the baseline was increased, but the detection of added $S_2O_3^{2-}$ was not affected (Figure 3A). Further, the detection limit of bimane- $S_2O_3^{2-}$ in the Tris-HCl buffer was improved to 10 nM by using the optimized conditions (Figure 3B).

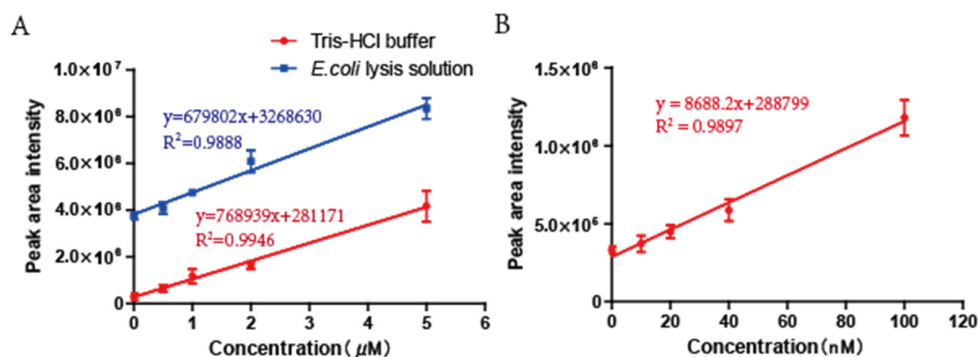


Figure 3. The standard curves of bimane- $S_2O_3^{2-}$ range at different concentrations. The standard curves of bimane- $S_2O_3^{2-}$ were established ranging from 0 to 5 μ M (A) and 0 to 0.1 μ M (B), respectively. The curve in blue color is plotted with cell lysate of *E. coli* BL21(DE3) as a complex background, and the curve in red color is plotted with Tris-HCl buffer as a plain background. Three parallel experiments were performed to obtain the averages and standard deviations ($n = 3$).

3.1. The Optimization of Bacterial Samples Preparation

E. coli iSS was tested by suspending the cells in the sample buffer (with SO_3^{2-}) and the control buffer (without SO_3^{2-}), and heating was used to convert iSS and SO_3^{2-} to $S_2O_3^{2-}$ [33]. Whether iSS was self-oxidized to $S_2O_3^{2-}$ during the heating process was tested by using DTT to reduce iSS to H_2S , as DTT readily reduces reactive sulfane sulfur, such as organic persulfide, to the corresponding thiol and H_2S [38]. *E. coli* cells were treated in the control buffer. When 0.2 mM DTT or more was added into the control buffer, $S_2O_3^{2-}$ in the control group decreased from 8.5×10^{-2} nmol/mL/OD to 1.5×10^{-2} nmol/mL/OD (Figure 4A). When $S_2O_3^{2-}$ was added to the control buffer, DTT did not reduce it after heating (Figure 4B). Thus, 0.5 mM DTT was subsequently included in the control buffer without SO_3^{2-} to prevent $S_2O_3^{2-}$ formation from the autoxidation of iSS during the heating process.

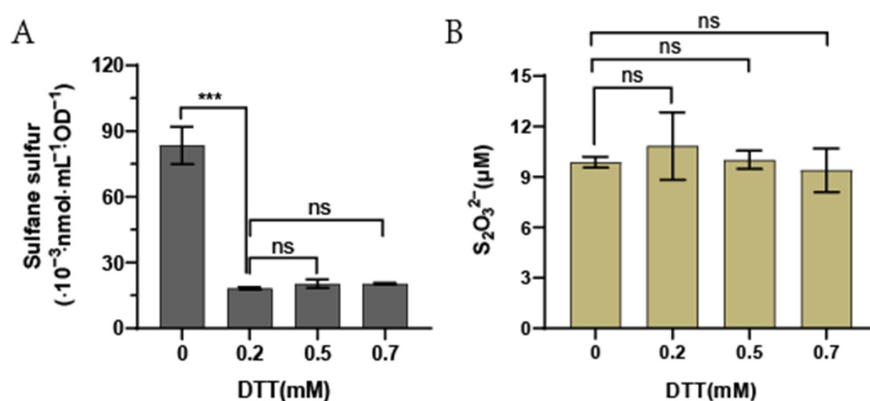


Figure 4. The addition of DTT in the control buffer prevented iSS formation from self-oxidation. (A) $S_2O_3^{2-}$ detected from 3 mL of *E. coli* BL21(DE3) cells at OD₆₀₀ of 1.0 resuspended in the control buffer with different amounts of DTT. (B) DTT did not reduce the amount of $S_2O_3^{2-}$. 10 μ M $S_2O_3^{2-}$ was dissolved in the control buffer with different amounts of DTT and heated at 95 °C for 10 min. The quantity of $S_2O_3^{2-}$ was determined after mBBR derivatization. Three parallel experiments were performed to obtain the averages and standard deviations (n = 3). The one-way ANOVA method was performed to calculate the *p*-values (Not significance (ns), *p* \geq 0.05; ***, *p* < 0.001).

Whether it is necessary to remove the residual culture supernatant before iSS determination was tested. Sulfane sulfur in the supernatant fluctuated around 23 μ M without significant changes during the growth of *E. coli* BL21(DE3) in the LB medium (Figure S1). When the harvested cells by centrifugation were washed once with Tris-HCl buffer (50 mM, pH = 7.4) as reported [33], iSS was 226.5 (10^{-3} nmol/mL/OD) (Figure 5A). When the harvested cells were directly measured without washing, iSS was 460.9 (10^{-3} ·nmol/mL/OD) (Figure 5A). The unwashed cell pellet contained several microliters of the culture supernatant, which contributed to the increased iSS. The residual supernatant was removed by second centrifugation to collect the liquid on the wall of the microfuge tube and pipetting removal (double-centrifugation step). With the double-centrifugation step, iSS was 281.1 (10^{-3} ·nmol/mL/OD) (Figure 5A). This double-centrifugation step was adopted because it minimizes the culture supernatant and prevents the loss of iSS during washing.

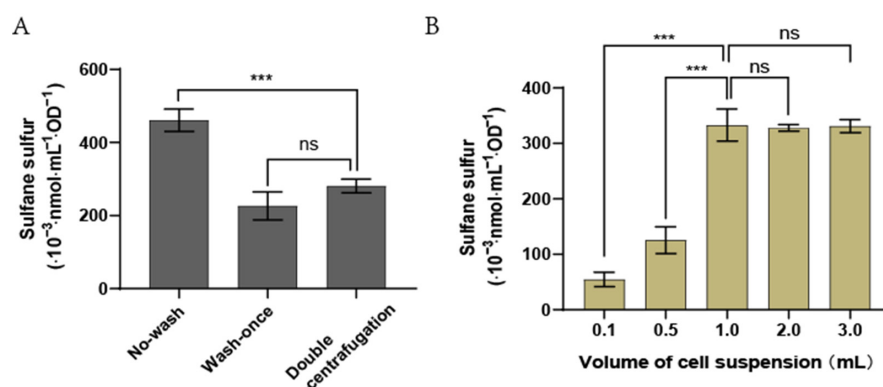


Figure 5. Effects of different treatment conditions on iSS content in *E. coli* cells. (A) The harvested cells were treated in three different ways. No-wash, the harvested cells directly proceeded for SdSS analysis without washing; wash-once, the harvested cells were washed once with 50 mM Tris-HCl (pH = 7.4); double-centrifugation, the cell pellets were re-centrifuged and the residual supernatant was removed. (B) Different volumes of cell suspension at OD₆₀₀ of 1.0 were harvested and analyzed by using the optimized method. Three parallel experiments were performed to obtain the averages and standard deviations (n = 3). The one-way ANOVA method was used to calculate the *p*-values (ns, *p* \geq 0.05; ***, *p* < 0.001).

Various volumes of an *E. coli* BL21(DE3) culture at OD₆₀₀ were used to detect iSS contents. With the revised method, iSS concentrations could be accurately detected with 1 mL of *E. coli* BL21(DE3) cells at OD₆₀₀ of 1.0, but the accuracy was reduced with sample volume smaller than 1 mL (Figure 5B). This optimized SdSS method was used in the following tests.

3.2. The Effects of Different Stress Factors on iSS Content of *E. coli*

When cell cultures of *E. coli* BL21(DE3) in LB medium were incubated at different temperatures for up to 30 min, the iSS contents were not significantly changed (Figure S2A). When cells were resuspended in LB or Tris-HCl buffer at different pH values, the iSS content in *E. coli* cells was not significantly changed (Figure S2B,C). 1–8% NaCl was added directly into the cultures to change the osmotic pressure, but it did not change the iSS content of cells, either (Figure S2D).

To test the effect of oxygen on iSS, the iSS content in *E. coli* was tested when the bacterium was cultured at different growth phases under both aerobic and anaerobic conditions. The iSS content under aerobic conditions rose to the highest level rapidly in the mid-log phase and remained high till the early stationary phase. It significantly decreased during the stationary phase (Figure 6A). However, under anaerobic conditions, the iSS content gradually increased during the entire log phase and reached its maximum in the early stationary phase. The high level of iSS content was relatively stable during the stationary phase (Figure 6B).

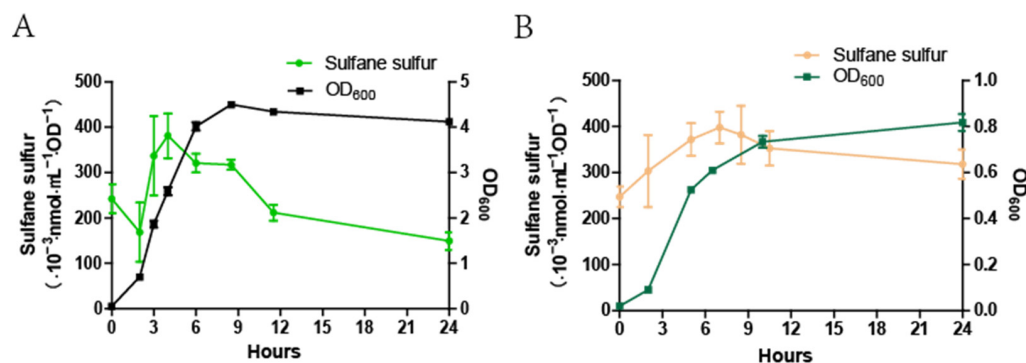


Figure 6. The iSS content of *E. coli* cells cultured under aerobic and anaerobic conditions. The *E. coli* BL21(DE3) cells were incubated in an LB medium and cultured under aerobic (A) and anaerobic conditions (B). The OD₆₀₀ and iSS content was detected at defined time intervals. Three parallel experiments for each condition were performed to obtain the averages and standard deviations (n = 3).

3.3. Effects of Cellular Redox Balance on *E. coli* iSS

Different compounds that could disturb the intracellular redox potential were used to test if they could change the homeostasis of sulfane sulfur in cells after 30-min treatment. DTT, TCEP, tBH, H₂O₂, sodium hypochlorite, diamide, and Fenton's reagent were tested at 1, 0.2, 0.25, 0.1, 0.1, 1, and 0.1 mM, respectively. CCCP and Rosup were used at 10 μM and 50 μg/mL. They are the reported concentrations in the literature and kit instruction [39–46]. Only CCCP and Rosup promoted iSS (Figure 7A). When tested at high concentrations, 10 mM Rosup, 10 mM diamide, and 5 mM Fenton's reagent increased iSS, but 10 mM H₂O₂ and tBH did not (Figure S3). For reductants, 1 mM DTT and 0.2 mM TCEP did not significantly change iSS (Figure 7A). When tested at high concentrations, 10 mM DTT reduced iSS, but 10 mM TCEP did not (Figure S3).

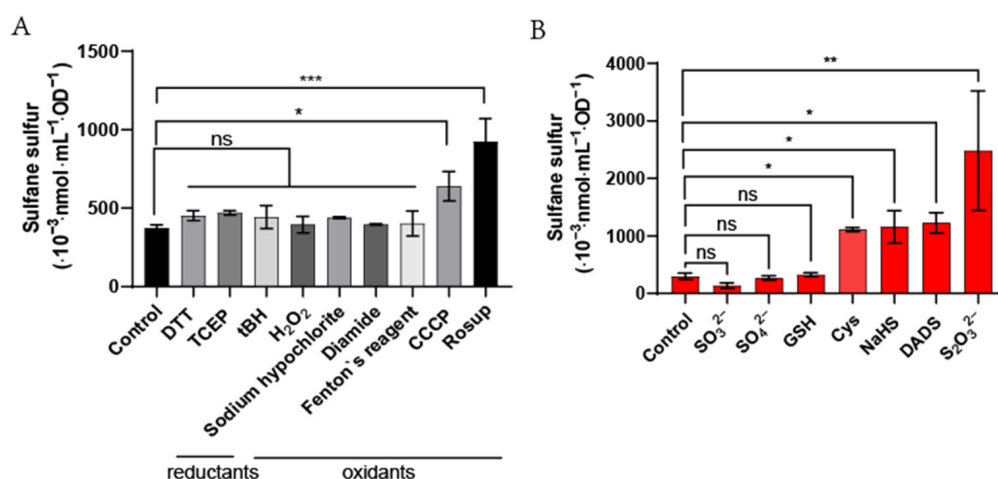


Figure 7. Changes in the iSS content of *E. coli* cells under different oxidants, reductants, and sulfur-bearing compounds. **(A)** *E. coli* BL21(DE3) cells were cultured until their OD₆₀₀ reached 1.0. Then, the cells were aliquoted, and different oxidants and reductants were added and incubated with them for 30 min before iSS detection. The DTT, TCEP, tBH, H₂O₂, sodium hypochlorite, diamide, Fenton's reagent, CCCP, and Rosup were used at 1, 0.2, 0.25, 0.1, 0.1, 1, 0.1 mM, 10 μ M, and 50 μ g/mL, respectively. **(B)** Different sulfur-bearing compounds at 10 mM were added and incubated with the cell cultures for 30 min before iSS detection. Three parallel experiments were performed to obtain the averages and standard deviations ($n = 3$). The One-way ANOVA method was performed to calculate the p -values (ns, $p \geq 0.05$; *, $p < 0.05$; **, $p < 0.01$; ***, $p < 0.001$).

3.4. Effects of Exogenous Sulfur-Bearing Compounds on *E. coli* iSS

Different sulfur-bearing compounds at 10 mM were added into *E. coli* BL21(DE3) cultures to test if they affected iSS. Cys, NaHS, DADS, and S₂O₃²⁻ increased the iSS content of *E. coli*, but GSH, SO₃²⁻ and SO₄²⁻ did not (Figure 7B). Low concentrations of S₂O₃²⁻, DADS, Cys, and NaHS were further tested, and they still increased iSS but at reduced magnitudes (Figure S4A–D). S₂O₃²⁻ was still the most effective, and it significantly increased iSS even at 0.5 mM.

The sulfur-bearing compounds which could promote iSS content were added to BL21(DE3) culture to observe whether they were toxic to cells at different concentrations. In a closed environment, all of these sulfur compounds except S₂O₃²⁻ repressed cell growth of *E. coli* to different degrees (Figure S5A–D). S₂O₃²⁻ at 10 mM or less did not show apparent inhibition. The DADS and NaHS showed more severe inhibition than Cys. In an open environment, the inhibition effect of DADS and NaHS was largely relieved (Figure S5F–H), likely because H₂S and DADS were volatile and evaporated. Again, S₂O₃²⁻ did not affect cell growth (Figure S5E).

Nontoxic S₂O₃²⁻ at 2 mM was added into the cell cultures of *E. coli* in LB medium to observe the change of iSS during growth. The iSS content greatly increased in comparison with the control (Figure 8). The iSS content reached the highest level at the end of logarithmic growth. Then it gradually decreased to a level similar to that of the control group after 24 h of growth.

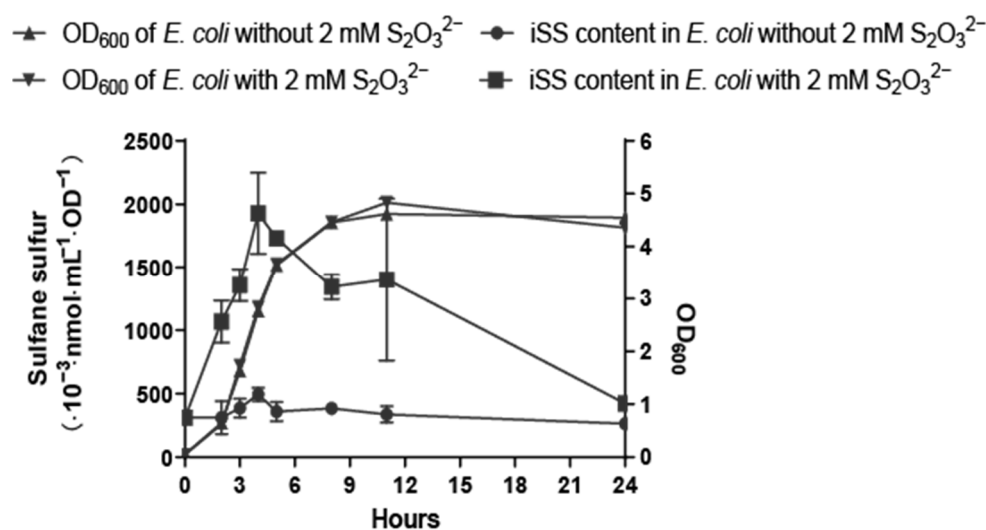


Figure 8. The addition of $S_2O_3^{2-}$ increased iSS contents in *E. coli* during growth in LB medium. *E. coli* BL21(DE3) cells were inoculated into fresh LB medium with or without 2 mM $S_2O_3^{2-}$ and cultured at 37 °C. The cells at defined time intervals were taken, and the OD₆₀₀ and iSS contents were determined. Three parallel experiments were performed to obtain the averages and standard deviations (n = 3).

4. Discussion

The previously reported SdSS method for iSS detection in bacteria was optimized. DTT is a key factor for optimization. DTT is a common reducing agent, and it reduces sulfane sulfur to H₂S [47]. The addition of DTT in the control buffer prevented the oxidation of iSS to thiosulfate, which interferes with the SdSS method. The inclusion of DTPA in both the reaction buffer and the control buffer is to chelate transition metals that catalyze sulfur oxidation [48]. Another improvement is the revised HPLC elution method. The revised method separates bimane- $S_2O_3^{2-}$ and bimane-GS so that the high concentrations of bimane-GS derived from *E. coli* will not interfere with bimane- $S_2O_3^{2-}$ detection (Figure 1B). Third, we optimized the fluorescence detection settings (Figures 1B and 2C and Table S1), and the detection threshold for bimane- $S_2O_3^{2-}$ was improved from 200 nM to 10 nM (Figure 3B). Finally, the double-centrifugation method to prepare cells before iSS detection was recommended (Figure 5A), as it minimizes culture supernatant and prevents the loss of iSS during washing with a buffer that changes the culturing environment of the tested cells.

We had expected a decrease in iSS when ROS was added to cell suspensions, as sulfane sulfur is known to react with ROS [49–51]; however, several tested reagents that induce oxidative stress increased iSS (Figure 7A). A possible explanation is that intracellular acid-labile sulfur is also oxidized by the addition of these reagents. The acid-labile sulfur, including Fe-S clusters, is sulfide [52,53]. When $O_2^{\bullet-}$ and $HO\bullet$ oxidize Fe-S clusters and release Fe^{2+} [54–56], the sulfur in the cluster is theoretically oxidized to sulfane sulfur (zero valences), as sulfide reacts with ROS to produce sulfane sulfur [57]. H_2O_2 and tBH were unable to increase iSS (Figure 7A), perhaps partly because they are rapidly metabolized by *E. coli* cells [58], partly because they react with sulfane sulfur at a relatively slow rate [40], and partly because they do not directly damage Fe-S clusters [59].

Sulfane sulfur, ROS, and Reactive chlorine species (RCS) are signaling molecules, and their signaling pathways may overlap [53,60,61]. OxyR is a major global regulator of *E. coli* in response to oxidative stress [62], and it also senses iSS through the persulfidation of Cys¹⁹⁹ [13]. Other redox-based transcriptional regulators also used Cys residues for signal sensing [61,63]. Two members of the MarR (multiple drug-resistant regulators) families that repress multiple drug efflux pumps have been shown to use Cys residues to sense both H_2O_2 and iSS [10,12]. Further, our data show that ROS and RCS significantly increased iSS in *E. coli* cells (Figure 7A). The results imply that iSS may participate in the signaling

transduction induced by ROS or RCS. Further studies are needed to understand whether sulfane sulfur is involved in the signaling induced by ROS and RCS.

$S_2O_3^{2-}$ is the only tested sulfur donor that could increase the iSS content without affecting bacterial growth (Figure S5 and Figure 8), and it may be used to increase iSS in *E. coli* or other organisms to evaluate the effect of elevated iSS on cells. Although $S_2O_3^{2-}$ may be used with other organisms to increase iSS, its concentration should be tested. For example, *Saccharomyces cerevisiae* is partially inhibited by 10 mM $S_2O_3^{2-}$, as high concentrations of $S_2O_3^{2-}$ directly inhibit cytochrome c oxidase of the electron transport chain in the yeast mitochondria [35]. *E. coli* is not inhibited by 10 mM $S_2O_3^{2-}$ (Figure 8), likely because it does not use cytochrome c oxidase in its electron transport chain [64]. There are two known metabolic pathways of $S_2O_3^{2-}$ in *E. coli*: one is catalyzed by CysM that uses $S_2O_3^{2-}$ to produce Cys [65,66], and Cys is then converted to sulfane sulfur [28]; the other is catalyzed by rhodanese (RHOD) GIpE that directly converts $S_2O_3^{2-}$ to sulfane sulfur [65]. *E. coli* contains eight proteins carrying RHOD domains [67]. Further studies are necessary to identify whether CysM or one or more RHODs are responsible to convert $S_2O_3^{2-}$ to sulfane sulfur.

In summary, we optimized the SdSS method and used *E. coli* as a model to extensively investigate the effects of different stress factors and reagents on iSS homeostasis. This work not only provides a better method for analyzing iSS in *E. coli* and possibly other biological samples but also investigated several factors possibly affecting iSS homeostasis, which facilitates further studies of the physiological functions of iSS.

Supplementary Materials: The following supporting information can be downloaded at: <https://www.mdpi.com/article/10.3390/antiox11071292/s1>, Figure S1: Sulfane sulfur concentrations in the supernatant of *E. coli* cultures growing in LB medium; Figure S2: The influence of temperature, pH, and osmolarity on iSS; Figure S3: Changes in the iSS content of *E. coli* cells under different oxidants; Figure S4: The iSS contents of *E. coli* BL21 (DE3) cells with varying concentrations of sulfur-bearing compounds; Figure S5: Growth curves of *E. coli* BL21(DE3) when incubated with different sulfur-bearing compounds; Table S1: Screening for best signal to noise ratio (SNR) of bimane- $S_2O_3^{2-}$ with the combinations of sensitivity and gain values.

Author Contributions: Conceptualization, Y.X. and L.X.; methodology, Y.X. and H.L.; investigation, Q.Y.; writing -original draft preparation, Q.Y.; validation, M.R.; formal analysis and sources, Y.Y.; project administration, Y.X. and L.X.; funding acquisition, Y.X. and L.X.; supervision, L.X. All authors have read and agreed to the published version of the manuscript.

Funding: The work was financially supported by grants from the National Natural Science Foundation of China (31870085, 91951202, 31961133015).

Institutional Review Board Statement: Not applicable.

Informed Consent Statement: Not applicable.

Data Availability Statement: All data are reported in the main text or Supplementary Data.

Conflicts of Interest: The authors declare no conflict of interest.

References

1. Mishanina, A.V.; Libiad, M.; Banerjee, R. Biogenesis of reactive sulfur species for signaling by hydrogen sulfide oxidation pathways. *Nat. Chem. Biol.* **2015**, *11*, 457–464. [CrossRef]
2. Kimura, H.; Shibuya, N.; Kimura, Y. Hydrogen Sulfide Is a Signaling Molecule and a Cytoprotectant. *Antioxid. Redox Signal.* **2012**, *17*, 45–57. [CrossRef]
3. Filipovic, M.R.; Zivanovic, J.; Alvarez, B.; Banerjee, R. Chemical Biology of H₂S Signaling through Persulfidation. *Chem. Rev.* **2018**, *118*, 377–461. [CrossRef]
4. Kimura, H. Hydrogen Sulfide (H₂S) and Polysulfide (H₂S)_n Signaling: The First 25 Years. *Biomolecules* **2021**, *11*, 896. [CrossRef]
5. Nagy, P.; Doka, E.; Ida, T.; Akaike, T. Measuring Reactive Sulfur Species and Thiol Oxidation States: Challenges and Cautions in Relation to Alkylation-Based Protocols. *Antioxid. Redox Signal.* **2020**, *33*, 1174–1189. [CrossRef]
6. Castelblanco, M.; Nasi, S.; Pasch, A.; So, A.; Busso, N. The role of the gasotransmitter hydrogen sulfide in pathological calcification. *Brit. J. Pharmacol.* **2020**, *177*, 778–792. [CrossRef]

7. Jarosz, A.P.; Wei, W.L.; Gauld, J.W.; Auld, J.; Ozcan, F.; Aslan, M.; Mutus, B. Glyceraldehyde 3-phosphate dehydrogenase (GAPDH) is inactivated by S-sulfuration in vitro. *Free Radic. Bio. Med.* **2015**, *89*, 512–521. [[CrossRef](#)]
8. Peng, H.; Zhang, Y.X.; Palmer, L.D.; Kehl-Fie, T.E.; Skaar, E.P.; Trinidad, J.C.; Giedroc, D.P. Hydrogen Sulfide and Reactive Sulfur Species Impact Proteome S-Sulphydration and Global Virulence Regulation in *Staphylococcus aureus*. *ACS Infect. Dis.* **2017**, *3*, 744–755. [[CrossRef](#)]
9. Mustafa, A.K.; Gadalla, M.M.; Sen, N.; Kim, S.; Mu, W.T.; Gazi, S.K.; Barrow, R.K.; Yang, G.D.; Wang, R.; Snyder, S.H. H₂S Signals Through Protein S-Sulphydration. *Sci. Signal.* **2009**, *2*, ra72. [[CrossRef](#)]
10. Xuan, G.; Lü, C.; Xu, H.; Chen, Z.; Li, K.; Liu, H.; Liu, H.; Xia, Y.; Xun, L. Sulfane Sulfur is an intrinsic signal activating MexR-regulated antibiotic resistance in *Pseudomonas aeruginosa*. *Mol. Microbiol.* **2020**, *114*, 1038–1048. [[CrossRef](#)]
11. Xuan, G.; Lv, C.; Xu, H.; Li, K.; Liu, H.; Xia, Y.; Xun, L. Sulfane Sulfur Regulates LasR-Mediated Quorum Sensing and Virulence in *Pseudomonas aeruginosa* PAO1. *Antioxidants* **2021**, *10*, 1498. [[CrossRef](#)]
12. Xu, H.; Xuan, G.; Liu, H.; Xia, Y.; Xun, L. Sulfane Sulfur Is a Strong Inducer of the Multiple Antibiotic Resistance Regulator MarR in *Escherichia coli*. *Antioxidants* **2021**, *10*, 1778. [[CrossRef](#)]
13. Hou, N.K.; Yan, Z.Z.; Fan, K.L.; Li, H.J.; Zhao, R.; Xia, Y.Z.; Xun, L.Y.; Liu, H.W. OxyR senses sulfane sulfur and activates the genes for its removal in *Escherichia coli*. *Redox Biol.* **2019**, *26*, 101293. [[CrossRef](#)]
14. Ni, X.; Kelly, S.S.; Xu, S.; Xian, M. The Path to Controlled Delivery of Reactive Sulfur Species. *Acc. Chem. Res.* **2021**, *54*, 3968–3978. [[CrossRef](#)]
15. Xu, S.; Hamsath, A.; Neill, D.L.; Wang, Y.Y.; Yang, C.T.; Xian, M. Strategies for the Design of Donors and Precursors of Reactive Sulfur Species. *Chem. Eur. J.* **2019**, *25*, 4005–4016. [[CrossRef](#)] [[PubMed](#)]
16. Gregory, G.J.; Boyd, E.F. Stressed out: Bacterial response to high salinity using compatible solute biosynthesis and uptake systems, lessons from Vibrionaceae. *Comput. Struct. Biotec.* **2021**, *19*, 1014–1027. [[CrossRef](#)]
17. Fang, F.C.; Frawley, E.R.; Tapscott, T.; Vazquez-Torres, A. Bacterial Stress Responses during Host Infection. *Cell Host Microbe* **2016**, *20*, 133–143. [[CrossRef](#)] [[PubMed](#)]
18. Reniere, M.L. Reduce, Induce, Thrive: Bacterial Redox Sensing during Pathogenesis. *J. Bacteriol.* **2018**, *200*, e00128-18. [[CrossRef](#)] [[PubMed](#)]
19. Lu, Z.; Imlay, J.A. When anaerobes encounter oxygen: Mechanisms of oxygen toxicity, tolerance and defence. *Nat. Rev. Microbiol.* **2021**, *19*, 774–785. [[CrossRef](#)]
20. Khademian, M.; Imlay, J.A. How Microbes Evolved to Tolerate Oxygen. *Trends Microbiol.* **2021**, *29*, 428–440. [[CrossRef](#)]
21. Reichmann, D.; Voth, W.; Jakob, U. Maintaining a Healthy Proteome during Oxidative Stress. *Mol. Cell* **2018**, *69*, 203–213. [[CrossRef](#)] [[PubMed](#)]
22. Zabel, M.; Nackenoff, A.; Kirsch, W.M.; Harrison, F.E.; Perry, G.; Schrag, M. Markers of oxidative damage to lipids, nucleic acids and proteins and antioxidant enzymes activities in Alzheimer’s disease brain: A meta-analysis in human pathological specimens. *Free Radic. Biol. Med.* **2018**, *115*, 351–360. [[CrossRef](#)] [[PubMed](#)]
23. Jakubczyk, K.; Dec, K.; Kaldunska, J.; Kawczuga, D.; Kochman, J.; Janda, K. Reactive oxygen species—Sources, functions, oxidative damage. *Pol. Merkur Lek.* **2020**, *48*, 124–127.
24. Ashby, L.V.; Springer, R.; Hampton, M.B.; Kettle, A.J.; Winterbourn, C.C. Evaluating the bactericidal action of hypochlorous acid in culture media. *Free Radic. Biol. Med.* **2020**, *159*, 119–124. [[CrossRef](#)] [[PubMed](#)]
25. Calleja, L.F.; Yoal-Sanchez, B.; Hernandez-Esquivel, L.; Gallardo-Perez, J.C.; Sosa-Garrocho, M.; Marin-Hernandez, A.; Jasso-Chavez, R.; Macias-Silva, M.; Rodriguez-Zavala, J.S. Activation of ALDH1A1 by omeprazole reduces cell oxidative stress damage. *FEBS J.* **2021**, *288*, 4064–4080. [[CrossRef](#)] [[PubMed](#)]
26. Corona, F.; Martinez, J.L.; Nikel, P.I. The global regulator Crc orchestrates the metabolic robustness underlying oxidative stress resistance in *Pseudomonas aeruginosa*. *Environ. Microbiol.* **2019**, *21*, 898–912. [[CrossRef](#)] [[PubMed](#)]
27. Di Simplicio, P.; Lupis, E.; Rossi, R. Different mechanisms of formation of glutathione-protein mixed disulfides of diamide and tert-butyl hydroperoxide in rat blood. *Biochim. Biophys. Acta* **1996**, *1289*, 252–260. [[CrossRef](#)]
28. Li, K.; Xin, Y.; Xuan, G.; Zhao, R.; Liu, H.; Xia, Y.; Xun, L. *Escherichia coli* Uses Separate Enzymes to Produce H₂S and Reactive Sulfane Sulfur From L-cysteine. *Front. Microbiol.* **2019**, *10*, 298. [[CrossRef](#)]
29. Pester, M.; Knorr, K.H.; Friedrich, M.W.; Wagner, M.; Loy, A. Sulfate-reducing microorganisms in wetlands—Fameless actors in carbon cycling and climate change. *Front. Microbiol.* **2012**, *3*, 72. [[CrossRef](#)]
30. Olson, K.R. H₂S and polysulfide metabolism: Conventional and unconventional pathways. *Biochem. Pharmacol.* **2018**, *149*, 77–90. [[CrossRef](#)]
31. Zhang, X.; Xin, Y.; Chen, Z.; Xia, Y.; Xun, L.; Liu, H. Sulfide-quinone oxidoreductase is required for cysteine synthesis and indispensable to mitochondrial health. *Redox Biol.* **2021**, *47*, 102169. [[CrossRef](#)] [[PubMed](#)]
32. Chiang, Y.H.; Jen, L.N.; Su, H.Y.; Lii, C.K.; Sheen, L.Y.; Liu, C.T. Effects of garlic oil and two of its major organosulfur compounds, diallyl disulfide and diallyl trisulfide, on intestinal damage in rats injected with endotoxin. *Toxicol. Appl. Pharm.* **2006**, *213*, 46–54. [[CrossRef](#)] [[PubMed](#)]
33. Ran, M.; Wang, T.; Shao, M.; Chen, Z.; Liu, H.; Xia, Y.; Xun, L. Sensitive Method for Reliable Quantification of Sulfane Sulfur in Biological Samples. *Anal. Chem.* **2019**, *91*, 11981–11986. [[CrossRef](#)] [[PubMed](#)]
34. Kruihof, P.D.; Lunev, S.; Lozano, S.P.A.; Batista, F.D.; Al-dahmani, Z.M.; Joles, J.A.; Dolga, A.M.; Groves, M.R.; van Goor, H. Unraveling the role of thiosulfate sulfurtransferase in metabolic diseases. *BBA Mol. Basis Dis.* **2020**, *1866*, 165716. [[CrossRef](#)] [[PubMed](#)]

35. Chen, Z.; Xia, Y.; Liu, H.; Liu, H.; Xun, L. The Mechanisms of Thiosulfate Toxicity against *Saccharomyces cerevisiae*. *Antioxidants* **2021**, *10*, 646. [[CrossRef](#)] [[PubMed](#)]
36. Lu, T.; Cao, Q.; Pang, X.; Xia, Y.; Xun, L.; Liu, H. Sulfane sulfur-activated actinorhodin production and sporulation is maintained by a natural gene circuit in *Streptomyces coelicolor*. *Microb. Biotechnol.* **2020**, *13*, 1917–1932. [[CrossRef](#)]
37. Müller, N.; Rauhut, D.; Tarasov, A. Sulfane Sulfur Compounds as Source of Reappearance of Reductive Off-Odors in Wine. *Fermentation* **2022**, *8*, 53. [[CrossRef](#)]
38. Kabil, O.; Banerjee, R. Redox Biochemistry of Hydrogen Sulfide. *J. Biol. Chem.* **2010**, *285*, 21903–21907. [[CrossRef](#)]
39. Park, Y.S.; Choi, S.E.; Koh, H.C. PGAM5 regulates PINK1/Parkin-mediated mitophagy via DRP1 in CCCP-induced mitochondrial dysfunction. *Toxicol. Lett.* **2018**, *284*, 120–128. [[CrossRef](#)]
40. Wang, Q.; Chen, Z.; Zhang, X.; Xin, Y.; Xia, Y.; Xun, L.; Liu, H. Rhodanese Rdl2 produces reactive sulfur species to protect mitochondria from reactive oxygen species. *Free Radic. Biol Med.* **2021**, *177*, 287–298. [[CrossRef](#)]
41. Huang, B.; Zhao, Z.; Huang, C.; Zhao, M.; Zhang, Y.; Liu, Y.; Liao, X.; Huang, S.; Zhao, Y. Role of metal cations and oxyanions in the regulation of protein arginine phosphatase activity of Yw1E from *Bacillus subtilis*. *Biochim. Biophys. Acta Gen. Subj.* **2020**, *1864*, 129698. [[CrossRef](#)]
42. Panmanee, W.; Charoenlap, N.; Atichartpongkul, S.; Mahavithakanont, A.; Whiteside, M.D.; Winsor, G.; Brinkman, F.S.L.; Mongkolsuk, S.; Hassett, D.J. The OxyR-regulated *phnW* gene encoding 2-aminoethylphosphonate: Pyruvate aminotransferase helps protect *Pseudomonas aeruginosa* from tert-butyl hydroperoxide. *PLoS ONE* **2017**, *12*, e0189066. [[CrossRef](#)] [[PubMed](#)]
43. Imlay, J.A. Where in the world do bacteria experience oxidative stress? *Environ. Microbiol.* **2019**, *21*, 521–530. [[CrossRef](#)] [[PubMed](#)]
44. Parker, B.W.; Schwessinger, E.A.; Jakob, U.; Gray, M.J. The RclR Protein Is a Reactive Chlorine-specific Transcription Factor in *Escherichia coli*. *J. Biol. Chem.* **2013**, *288*, 32574–32584. [[CrossRef](#)] [[PubMed](#)]
45. Bakovic, J.; Yu, B.Y.K.; Silva, D.; Baczynska, M.; Peak-Chew, S.Y.; Switzer, A.; Burchell, L.; Wigneshweraraj, S.; Vandanashree, M.; Gopal, B.; et al. Redox Regulation of the Quorum-sensing Transcription Factor AgrA by Coenzyme, A. *Antioxidants* **2021**, *10*, 841. [[CrossRef](#)] [[PubMed](#)]
46. Spear, N.; Aust, S.D. Effects of glutathione on Fenton reagent-dependent radical production and DNA oxidation. *Arch. Biochem. Biophys.* **1995**, *324*, 111–116. [[CrossRef](#)]
47. Miyamoto, R.; Koike, S.; Takano, Y.; Shibuya, N.; Kimura, Y.; Hanaoka, K.; Urano, Y.; Ogasawara, Y.; Kimura, H. Polysulfides (H₂Sn) produced from the interaction of hydrogen sulfide (H₂S) and nitric oxide (NO) activate TRPA1 channels. *Sci. Rep.* **2017**, *7*, 45995. [[CrossRef](#)]
48. Stevens, R.; Stevens, L.; Price, N.C. The Stabilities of Various Thiol Compounds Used in Protein Purifications. *Biochem. Educ.* **1983**, *11*, 70. [[CrossRef](#)]
49. Olson, K.R. Hydrogen sulfide, reactive sulfur species and coping with reactive oxygen species. *Free Radical Bio. Med.* **2019**, *140*, 74–83. [[CrossRef](#)]
50. Hancock, J.T.; Whiteman, M. Hydrogen sulfide signaling: Interactions with nitric oxide and reactive oxygen species. *Ann. N. Y. Acad. Sci.* **2016**, *1365*, 5–14. [[CrossRef](#)]
51. Fukuto, J.M.; Ignarro, L.J.; Nagy, P.; Wink, D.A.; Kevil, C.G.; Feelisch, M.; Cortese-Krott, M.M.; Bianco, C.L.; Kumagai, Y.; Hobbs, A.J.; et al. Biological hydropersulfides and related polysulfides—A new concept and perspective in redox biology. *FEBS Lett.* **2018**, *592*, 2140–2152. [[CrossRef](#)] [[PubMed](#)]
52. Predmore, B.L.; Lefer, D.J.; Gojon, G. Hydrogen Sulfide in Biochemistry and Medicine. *Antioxid. Redox Signal.* **2012**, *17*, 119–140. [[CrossRef](#)] [[PubMed](#)]
53. Iciek, M.; Bilska-Wilkosz, A.; Gorny, M. Sulfane sulfur—New findings on an old topic. *Acta Biochim. Pol.* **2019**, *66*, 533–544. [[CrossRef](#)]
54. Bruska, M.K.; Stiebritz, M.T.; Reiher, M. Binding of Reactive Oxygen Species at Fe-S Cubane Clusters. *Chem. A Eur. J.* **2015**, *21*, 19081–19089. [[CrossRef](#)]
55. Lu, Z.; Imlay, J.A. A conserved motif liganding the [4Fe-4S] cluster in [4Fe-4S] fumarases prevents irreversible inactivation of the enzyme during hydrogen peroxide stress. *Redox Biol.* **2019**, *26*, 101296. [[CrossRef](#)]
56. Rydz, L.; Wrobel, M.; Jurkowska, H. Sulfur Administration in Fe-S Cluster Homeostasis. *Antioxidants* **2021**, *10*, 1738. [[CrossRef](#)] [[PubMed](#)]
57. Bian, J.S.; Olson, K.R.; Zhu, Y.C. Hydrogen Sulfide: Biogenesis, Physiology, and Pathology. *Oxid. Med. Cell. Longev.* **2016**, *2016*, 6549625. [[CrossRef](#)] [[PubMed](#)]
58. Mishra, S.; Imlay, J. Why do bacteria use so many enzymes to scavenge hydrogen peroxide? *Arch. Biochem. Biophys.* **2012**, *525*, 145–160. [[CrossRef](#)] [[PubMed](#)]
59. Flint, D.H.; Tuminello, J.F.; Emptage, M.H. The inactivation of Fe-S cluster containing hydro-lyases by superoxide. *J. Biol. Chem.* **1993**, *268*, 22369–22376. [[CrossRef](#)]
60. Gray, M.J.; Wholey, W.Y.; Jakob, U. Bacterial Responses to Reactive Chlorine Species. *Annu. Rev. Microbiol.* **2013**, *67*, 141–160. [[CrossRef](#)]
61. Sevilla, E.; Bes, M.T.; Gonzalez, A.; Peleato, M.L.; Fillat, M.F. Redox-Based Transcriptional Regulation in Prokaryotes: Revisiting Model Mechanisms. *Antioxid. Redox Signal.* **2019**, *30*, 1651–1696. [[CrossRef](#)] [[PubMed](#)]
62. Chiang, S.M.; Schellhorn, H.E. Regulators of oxidative stress response genes in *Escherichia coli* and their functional conservation in bacteria. *Arch. Biochem. Biophys.* **2012**, *525*, 161–169. [[CrossRef](#)] [[PubMed](#)]

63. Lee, I.G.; Lee, B.J. How Bacterial Redox Sensors Transmit Redox Signals via Structural Changes. *Antioxidants* **2021**, *10*, 502. [[CrossRef](#)]
64. Uden, G.; Bongaerts, J. Alternative respiratory pathways of Escherichia coli: Energetics and transcriptional regulation in response to electron acceptors. *BBA Bioenergetics* **1997**, *1320*, 217–234. [[CrossRef](#)]
65. Kawano, Y.; Onishi, F.; Shiroyama, M.; Miura, M.; Tanaka, N.; Oshiro, S.; Nonaka, G.; Nakanishi, T.; Ohtsu, I. Improved fermentative L-cysteine overproduction by enhancing a newly identified thiosulfate assimilation pathway in Escherichia coli. *Appl. Microbiol. Biot.* **2017**, *101*, 6879–6889. [[CrossRef](#)]
66. Sirko, A.; Hryniewicz, M.; Hulanicka, D.; Bock, A. Sulfate and Thiosulfate Transport in Escherichia-Coli K-12—Nucleotide-Sequence and Expression of the Cystwam Gene-Cluster. *J. Bacteriol.* **1990**, *172*, 3351–3357. [[CrossRef](#)] [[PubMed](#)]
67. Cheng, H.; Donahue, J.L.; Battle, S.E.; Ray, W.K.; Larson, T.J. Biochemical and Genetic Characterization of PspE and GlpE, Two Single-domain Sulfurtransferases of Escherichia coli. *Open Microbiol. J.* **2008**, *2*, 18–28. [[CrossRef](#)]